Thermal emission of spinning photons from temperature gradients

P. Y. Chen,[1,*] C. Khandekar,[2] R. Ayash,[1] Z. Jacob,[2] and Y. Sivan[1]

[1]*School of Electrical and Computer Engineering, Ben-Gurion University of the Negev*

[2]*School of Electrical and Computer Engineering, Purdue University*

(Dated: 9th May 2022)

Abstract

The fluctuational electrodynamic investigation of thermal radiation from non-equilibrium or non-isothermal bodies remains largely unexplored because it necessarily requires volume integration over the fluctuating currents inside the emitter which quickly becomes computationally intractable. Here, we put forth a formalism combining fast calculations based on modal expansion and fluctuational electrodynamics to accelerate research at this frontier. We employ our formalism on a sample problem: a long silica wire held under temperature gradient within its cross section. We discover that the far-field thermal emission carries a nonzero spin which is constant in direction and sign, and interestingly, is transverse to the direction of the power flow. We clearly establish the origin of this transverse spin as arising from the nonequilibrium intermixing of the cylindrical modes of the wire, and not from any previously studied or intuitively expected origins such as chiral or nonisotropic materials and geometries, magnetic materials or fields, and mechanical rotations. This finding of nonequilibrium spin texture of emitted heat radiation can prove useful for advancing the noninvasive thermal metrology or infrared imaging techniques.

Keywords: thermal radiation; temperature gradients; photon spin; longitudinal and transverse spin; modal expansion for computational electromagnetics; eigenpermittivity modes

I. INTRODUCTION

The field of thermal radiation initiated the quantum revolution at the beginning of the twentieth century and spawned numerous technological applications such as thermal energy harvesting, infrared imaging, metrology, gas sensing, and heat management, among others [1–4]. One emerging research direction focuses on the spin angular momentum or circular polarization of thermal radiation. The key guiding principle for this research has been the photon-spin-resolved Kirchhoff's law, which equates emissivity with absorptivity separately for individual circular polarization states of thermally emitted light. However, this law is derived and applicable only to uniform-temperature reciprocal media [5–7]. While recent works have explored the spin angular momentum of thermal radiation from time-reversal-symmetry-broken nonreciprocal media [8–10], it remains an open question whether nonuniform temperature profiles can lead to interesting effects on the circular polarization of thermal emission.

In this work, we develop the theoretical and computational framework to analyze the spin angular momentum of thermal radiation from bodies with non-

* parryyu@post.bgu.ac.il

uniform temperature profiles. As an experimentally-relevant example, we consider a long cylindrical rod with a non-uniform temperature distribution across its cross-section. Our analysis is performed by extending the recently developed techniques for rapid simulation of Green's function [11–13] to thermal radiation. Crucially, we focus on the spin angular momentum rather than the radiative heat flux. Shown in the left panel of Fig. 1, a long (silica, SiO_2) rod is held under a linear temperature gradient. We find that, in the far-field, the heat flux is radially outward, but there also exists a non-zero spin angular momentum density parallel to the axis of the cylinder and transverse to the emission direction. The left panel also shows the sense of polarization rotation associated with the dimensionless spin, while the right panel displays its magnitude, with blue/red indicating positive/negative directionality. With detailed analysis, we prove that this transverse spin is uniquely enabled by the non-uniform temperature distributions and arises from the intermixing of contributions from different cylindrical modes. We also show numerically that the spin magnitude diminishes with diminishing temperature gradient, falling to zero for a uniform temperature profile (Figure 2).

Until recently, inquiries into the nature of spin arising from thermal radiation were limited to reciprocal media, focusing on two major themes: far-field spin from reciprocal chiral absorbers explored theoretically [14, 15] and experimentally [16, 17], and the analysis of the degree of polarization in the near-field of reciprocal media [18]. Recent exploration of this topic for non-reciprocal media has revealed surprising phenomena, such as persistent equilibrium spin in the near-field [19] and modified spin-resolved Kirchhoff's laws for planar media [20]. Ref. [21] revealed an origin of far-field thermal-radiation spin: a nonequilibrium system composed of a dimer of two coupled antennas held at unequal but uniform or homogeneous temperatures. Along this vein, our work demonstrates a fundamentally new finding that even nonuniform temperature gradients inside a single thermal emitter can cause thermal emission with a nonzero spin. Our specific example system lacks all previously known aspects connected with the photon spin such as geometric chirality (e.g. nonsymmetrical shapes), material chirality (e.g. chiral or anisotropic materials), magnetic field or magnetic materials, and mechanical rotations. By avoiding these aspects, our work clearly establishes a surprising connection between the nonzero photon spin and the intrinsic temperature gradients. We also note that, in contrast to all previous works reporting longitudinal spin, the far-field spin emitted from the temperature gradient emitter is transverse in nature, thus, making it measurable for greater ease; in fact, such transverse spin was so far believed to be possible only in the near-field. We further highlight that the physical origin of this spin is based on non-equilibrium intermixing of cylindrical modes of different orders, which differs from that of Ref. [21], where it stems from the near-field coupling between non-parallel dipole moments.

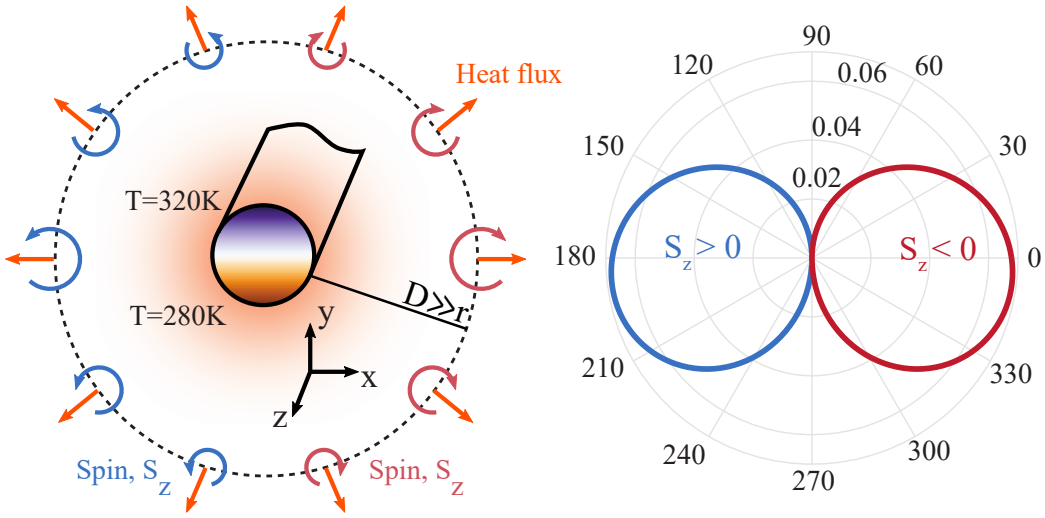

Figure 1: (Left) An example geometry that can be treated by our formalism for non-equilibrium fluctuation electrodynamics. A temperature gradient is maintained across the cross-section of a circular silica rod, which extends infinitely along the z-direction. Heat flux, characterized by Poynting's vector, is generated along the radial direction. More notably, spin fields are generated that are in-plane, characterized by a spin vector which is perpendicular to both the plane and the Poynting vector. (Right) The spin extends into the far-field, $D \gg r$, where r is the radius of the cylinder and D is the radius of the far-field contour. The normalized quantity $\langle S_z \rangle \omega / \langle W \rangle$ converges to the displayed non-zero values. The sign and the magnitude of the far-field spin vector changes as a function of the in-plane polar angle, but does not substantially change at scales of the order of the wavelength.

Fluctuation-electrodynamic (FE) simulations of thermal radiation from emitters with non-uniform or continuously varying temperature/material profiles necessarily require volume integrals over fluctuating currents, and precludes simplification to surface integrals; the surface current formulations that apply to uniform temperature/material profiles [22–24] are inapplicable here. Note also that there is no Kirchhoff's law for bodies with nonuniform temperature profiles. While Kirchhoff's law can be generalized for differential subvolumes of reciprocal bodies [1], it does not circumvent the need for volume integration for the calculation of the total far-field thermal radiation spin from such nonisothermal emitters. For volume currents, a formulation was recently developed for emitters with internal inhomogeneities [25], and a new approach to tailor the directionality and intensity of thermal emission using temperature gradients was explored in Ref. [26]. These works presented successful but specific numerical techniques. In the present work,

we instead aim to develop a general formalism for spatially-varying temperature profiles that is compatible with any simulation method. There have been many recent works on thermal radiation in systems of sub-wavelength particles where the particles can be approximated as point dipoles, thus simplifying the FE simulations and analysis [7, 27–29]. Our approach ventures beyond the dipolar regime, paving the way for computationally challenging FE simulations of many-body non-dipolar systems.

We employ a modal expansion approach that decomposes the radiation of emitters via their resonator modes. The primary advantage is that once the modes have been obtained using any readily available mode-solver, it is computationally inexpensive to analyze the thermal radiation of any temperature profile. This speed is conducive to complex heat-transfer simulations between bodies with non-uniform temperature distributions requiring self-consistent analysis in presence of other heat-transfer channels like conduction and convection. Furthermore, modal expansion yields useful insights regarding spectral, geometric, and symmetry properties. For example, we can deduce which combination of modes gives rise to non-zero spin simply by considering the spatial overlap between the temperature profile and modal fields. Such insights and design tools are not readily accessible to purely numerical methods such as volume current formulations.

We note that modal expansion was recently used in the form of temporal coupled mode theory (CMT) in Refs [30, 31] to engineer the directionality of Poynting flux. Instead of the eigenfrequency modes employed by CMT, our modal expansion uses eigenpermittivity modes, which offers several advantages. Firstly, eigenpermittivity modes form a discrete set, which is simpler to treat numerically compared with the continuum of frequency modes. Crucially, our formalism can handle temperature inhomogeneities within the spatial extent of a single mode, which is inaccessible to CMT utilizing a single effective mode temperature [30, 31]. Furthermore, our formalism is suitable for direct simulation of hybridized or strongly coupled modes in the context of many-body heat-transfer simulations, which for the CMT formalism would require parameter extraction based on numerical fitting beyond the weak-coupling regime. Another advantage of our approach is that the frequencies used for the Planck factor (see Eq. (4) below; the mean energy of an electromagnetic state) are real, thus, avoiding any approximation necessary for complex frequency modes.

II. FORMULATION

We now develop the formulation for the fields emitted by an arbitrary hot object standing in an optically and thermally uniform background. We assume that the

object contains thermal emitters that create a fluctuating current density $\boldsymbol{J}(\boldsymbol{r}')$. The total electric and magnetic fields at point $\boldsymbol{r}$ exterior to the object due to the current $\boldsymbol{J}(\boldsymbol{r}')$ are

$$E_l(\boldsymbol{r}) = ikZ_0 \int d\boldsymbol{r}' G^E_{lq}(\boldsymbol{r},\boldsymbol{r}') J_q(\boldsymbol{r}'), \qquad H_l(\boldsymbol{r})/Z_0 = ik \int d\boldsymbol{r}' G^H_{lq}(\boldsymbol{r},\boldsymbol{r}') J_q(\boldsymbol{r}'), \tag{1}$$

where $Z_0 = \sqrt{\mu_0/\epsilon_0}$ is the free space impedance. For convenience, we rescale the magnetic field, such that $\boldsymbol{H} = Z_0 \boldsymbol{H}^{\mathrm{SI}}$, where $\boldsymbol{H}^{SI}$ is the SI quantity. Here, $\bar{\bar{G}}^E(\boldsymbol{r},\boldsymbol{r}')$ and $\bar{\bar{G}}^H(\boldsymbol{r},\boldsymbol{r}')$ are the Green's tensors for electric and magnetic fields. They are related through $\bar{\bar{G}}^H(\boldsymbol{r},\boldsymbol{r}') = \frac{1}{ik}\nabla \times \bar{\bar{G}}^E(\boldsymbol{r},\boldsymbol{r}')$. The electromagnetic properties of the medium are encoded within the Green's tensors.

Our facile yet rigorous treatment of varying temperature profiles is enabled by the expansions

$$\bar{\bar{G}}^E(\boldsymbol{r},\boldsymbol{r}') = \frac{1}{k^2}\sum_m \frac{\boldsymbol{E}^m(\boldsymbol{r}) \otimes \boldsymbol{E}^{m,\dagger}(\boldsymbol{r}')}{\epsilon_m - \epsilon_i} \qquad \bar{\bar{G}}^H(\boldsymbol{r},\boldsymbol{r}') = \frac{1}{k^2}\sum_m \frac{\boldsymbol{H}^m(\boldsymbol{r}) \otimes \boldsymbol{E}^{m,\dagger}(\boldsymbol{r}')}{\epsilon_m - \epsilon_i}, \tag{2}$$

where ϵ_m are the eigenpermittivities associated with the eigenmodes $\boldsymbol{E}^m(\boldsymbol{r})$, and ϵ_i is the permittivity of the object. Notice that the dependence on $\boldsymbol{r}$ and $\boldsymbol{r}'$ has been separated into the factors $\boldsymbol{E}^m(\boldsymbol{r})$ and $\boldsymbol{E}^{m,\dagger}(\boldsymbol{r}')$, a key feature that we shall later exploit. This simple form differs from the expansion derived in earlier eigenpermittivity formulations [11, 32], since it applies when the source co-ordinate $\boldsymbol{r}'$ is inside the object. Its derivation is given in Section I Suppl. Mat., along with a short discussion.

We shall employ the Fluctuation-Dissipation Theorem (FDT) [33, 34] to calculate the fields produced by ensemble averages of fluctuating currents; products of fluctuating currents are correlated and satisfy

$$\langle J_p(\boldsymbol{r}',\omega') J^*_q(\boldsymbol{r}'',\omega'')\rangle = \frac{4\omega\epsilon_0}{\pi}\Theta(\omega,T)\,\mathrm{Im}[\epsilon(\boldsymbol{r}')]\delta(\boldsymbol{r}'-\boldsymbol{r}'')\delta(\omega'-\omega'')\delta_{pq}, \tag{3}$$

where

$$\Theta(\omega,T) = \frac{\hbar\omega}{e^{\hbar\omega/k_BT}-1}, \tag{4}$$

is the mean energy of an electromagnetic state at temperature T, and $\langle\rangle$ represents ensemble averaging.

We aim to evaluate various field quantities such as the Poynting flux,

$$\langle P_i(\boldsymbol{r},\omega)\rangle = \frac{1}{2Z_0}\epsilon_{ilp}\,\mathrm{Re}\langle E^*_l H_p\rangle, \tag{5}$$

rewritten using tensor notation, with ϵ_{ilp} being the Levi-Civita symbol for the cross-product, and the $\boldsymbol{H}$ field is rescaled. Two additional key quantities are the spin momentum density,

$$\langle S_i(\boldsymbol{r},\omega)\rangle = \frac{\epsilon_{ilp}}{2Z_0kc^2}\,\mathrm{Im}\left\{\langle E_l^* E_p\rangle + \langle H_l^* H_p\rangle\right\}, \tag{6}$$

and the energy density,

$$\langle W(\boldsymbol{R},\omega)\rangle = \frac{\delta_{lp}}{2Z_0c}\left\{\langle E_l^* E_p\rangle + \langle H_l^* H_p\rangle\right\}, \tag{7}$$

where δ_{lp} is the Kronecker delta. Other quantities such as Stokes' parameters can also be considered.

To treat this range of quantities, we consider the general tensor element $\langle D_l^* F_p\rangle$, where D_l^* and F_p can represent either $\boldsymbol{E}$ or $\boldsymbol{H}$. The result for cylinders of arbitrary cross-section is derived in Section II Suppl. Mat., and is

$$\langle D_l^* F_p\rangle = \frac{2Z_0\epsilon_i''(\omega)}{\pi^2 k}\int_{-k}^{k} d\beta \sum_{m,n} D_l^{m,*}(\boldsymbol{R})F_p^n(\boldsymbol{R})\frac{V^{m,n}}{d^{m,n}}, \tag{8}$$

defining the two quantities

$$V^{m,n} = \int d\boldsymbol{R}'\Theta(\omega,T)\boldsymbol{E}^{m,\dagger,*}(\boldsymbol{R}')\cdot\boldsymbol{E}^{n,\dagger}(\boldsymbol{R}'), \tag{9}$$

$$d^{m,n} = (\epsilon_m-\epsilon_i)^*(\epsilon_n-\epsilon_i). \tag{10}$$

Equation (8) gives the fields radiated by thermal emission at ω per unit length of a 2D geometry standing in free space. As an aside, the equivalent result for 3D structures is displayed in Eq. (14) Suppl. Mat.. The 3D result is simpler than Eq. (8), as no integration along β is necessary since all information pertaining to field profiles is captured by the modes themselves.

The product (8) can represent energy flux (5) or energy density (7), for example. We choose to limit the integral over the longitudinal propagation constant β to the propagating Fourier components, see Eq. (15) Suppl. Mat.. The summations over indices m and n run over the same set of modes, as per Eq. (17) Suppl. Mat.. We see that Eq. (8) is composed of three parts. First, the factor $d^{m,n}$ is due to the detuning of the inclusion permittivity ϵ_i from the eigenpermittivities ϵ_m of each mode. Second, the integral $V^{m,n}$ over the electric fields of the eigenmodes $\boldsymbol{E}^{m,\dagger,*}(\boldsymbol{R}')\cdot\boldsymbol{E}^{n,\dagger}(\boldsymbol{R}')$ within the interior of the inclusion is ultimately weighted by the temperature profile. The variable $\boldsymbol{R}=(x,y)$ ranges over the 2D plane. Finally, the result is given by a sum over the eigenmodal fields $D_l^{m,*}(\boldsymbol{R})F_p^n(\boldsymbol{R})$ in the region exterior to the inclusion.

The computational advantage of Eq. (8) is that once the modes of the resonator have been obtained, many quantities of interest regarding the radiation are available by evaluating just the one set of overlap integrals. Even the difficult case of non-uniform temperature profiles can be treated with relative ease. This greatly facilitates any calculation that requires iteration over many temperature profiles, such as self-consistent calculations.

When Eq. (8) is applied to find the Poynting vector (5), we obtain

$$\langle \boldsymbol{P}(\boldsymbol{R},\omega)\rangle = \frac{\epsilon_i''(\omega)}{\pi^2 k}\int_{-k}^{k} d\beta \sum_{m,n} \mathrm{Re}\left\{ \boldsymbol{E}^{m,*}(\boldsymbol{R}) \times \boldsymbol{H}^{n}(\boldsymbol{R}) \frac{V^{m,n}}{d^{m,n}} \right\}. \tag{11}$$

The spin momentum density (6) is obtained by applying (8) twice,

$$\langle \boldsymbol{S}(\boldsymbol{R},\omega)\rangle = \frac{\epsilon_i''(\omega)}{\pi^2 k^2 c^2}\int_{-k}^{k} d\beta \sum_{m,n} \mathrm{Im}\left\{ (\boldsymbol{E}^{m,*} \times \boldsymbol{E}^{n} + \boldsymbol{H}^{m,*} \times \boldsymbol{H}^{n}) \frac{V^{m,n}}{d^{m,n}} \right\}. \tag{12}$$

Also, the energy density (7) is

$$\langle W(\boldsymbol{R},\omega)\rangle = \frac{\epsilon_i''(\omega)}{\pi^2 k c}\int_{-k}^{k} d\beta \sum_{m,n} (\boldsymbol{E}^{m,*} \cdot \boldsymbol{E}^{n} + \boldsymbol{H}^{m,*} \cdot \boldsymbol{H}^{n}) \frac{V^{m,n}}{d^{m,n}}. \tag{13}$$

The formalism developed above has been validated against other methods from the literature [35]; see Section IV Suppl. Mat..

III. RESULTS

We use the formalism in Section II to treat radiation from a long cylinder with a temperature gradient. Though the geometry is simple, the radiated fields nevertheless exhibit a non-trivial structure. Consider a circular SiO_2 rod of radius $r = 4.5\mu$m. We focus on its radiation at a wavelength of 9.4 μm, where SiO_2 is at resonance and has a permittivity of approximately $-3.19 + 4.97i$. The rod rests in a vacuum background at zero temperature. For this geometry, the eigenmodes $\{\boldsymbol{E}^m\}$ are available analytically (see [11]), while their eigenvalues $\{\epsilon_m\}$ can be found via a root search [12]. Thus, to use (8), we need only integrate over β and specify a temperature profile. In the results that follow, we shall integrate over only the propagating orders, where $\beta < \omega/c$. This means that near-fields—within one or two wavelengths of the cylinder—may be inaccurate.

When the cylinder is set to a uniform temperature of 300 K, the cylinder produces rotationally invariant thermal radiation: a Poynting flux oriented in the radial direction. All components of spin are zero, corresponding to the origin of

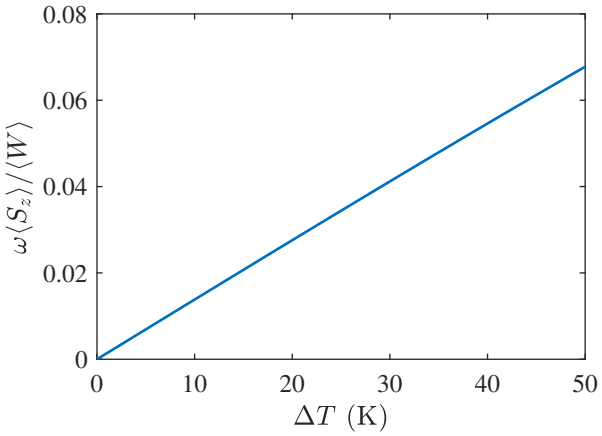

Figure 2: The magnitude of the far-field spin generated by thermal emission is approximately linearly proportional to the temperature gradient. Along the horizontal axis, the size of ΔT varies, defined by the hottest and coldest points of the rod in Figure 3. The vertical axis is the resulting normalized spin density.

Figure 2. When a linear temperature gradient is introduced, of the type shown in Figure 3 (a), the profile of the radiated Poynting flux remains largely rotationally invariant (Figure 1 in the Suppl. Mat.). However, a small but measurable axial component of spin appears, oriented along the z-axis (Figure 1), which is transverse to the radial energy flux. As such, this spin cannot be classified as circular polarization, since the spin axis and Poynting vector do not align. In Figure 3 (b), we plot the spatial profile of this spin, normalized by the energy density, $\langle S_z\rangle\omega/\langle W\rangle$. A plane of symmetry exists in the spin profile, which originates from the symmetry of the temperature profile. However, the sign of the spin is inverted about this plane, since spin is a pseudovector. We also observe in Figure 3 (c) that this spin extends into the far-field, where its strength remains undiminished.

These kinds of observations generalize to other temperature gradients. For example, the temperature gradient of Figure 4 (a) contains two planes of symmetry. A non-zero spin is produced, Figure 4 (b), containing these two planes of symmetry. Once again, the spin extends into the far-field (Figure 4 (c)), but with a smaller magnitude relative to the linear temperature gradient. Crucially, changes to the temperature gradient induce both qualitative and quantitative changes to the far-field spin pattern. By contrast, temperature gradients do not induce any qualitative changes to the far-field Poynting flux, which remains circularly symmetric to zeroth order, as evidenced by Figure 1 Suppl. Mat.. Thus, the far-field spin may enable non-destructive measurement of an emitter's temperature profile.

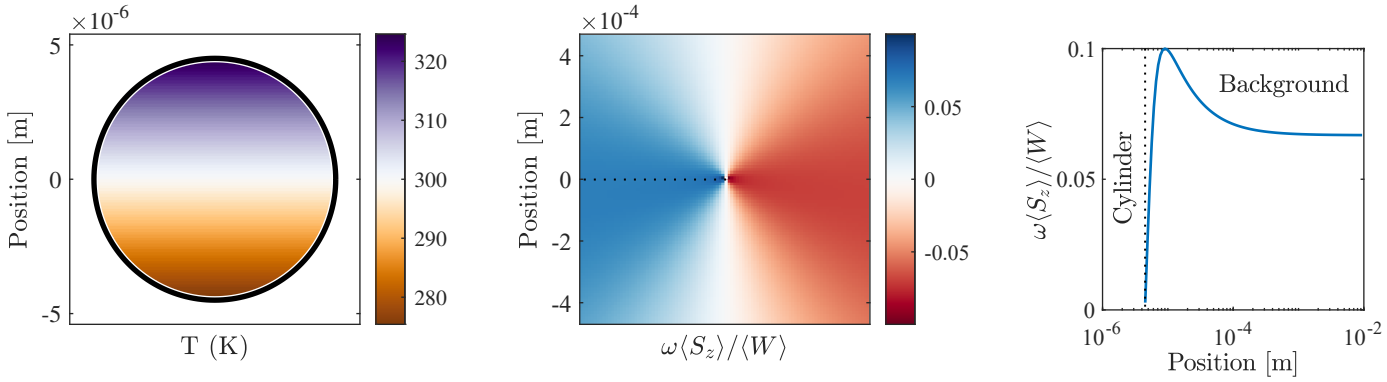

(a) (b) (c)

Figure 3: Emission from a linear temperature gradient. (a) Temperature profile across the cross-section of the rod standing in vacuum, featuring the same linear gradient as Figure 1. (b) Axial spin generated by the radiating rod (S_z normalized by W). In this xy-plane, there exists a plane of symmetry that coincides with the temperature profile. A different view of the angular variation of S_z is presented in Figure 1. (c) Axial spin (normalized by W), with a strength that does not diminish into the far-field; ; the maximal values of the spin are obtained already about a wavelength away from the rod center, so that the role of the evanescent modes (which are not calculated) are expected to have, at most, a small effect on them. The trajectory for the x-axis is along the dotted line of subfigure (b) (i.e., $x < 0, y = 0$). The plot domain changes drastically across the subfigures.

IV. DISCUSSION

In this paper, the modal formalism not only provides an efficient means of calculating thermal radiation, especially from spatially varying temperature profiles, but also provides insight into its behaviour. For example, we can identify the origins of the non-zero spin, yielding insights into symmetry and spectral properties. From (12), the spin pattern is determined by products of pairs of modes, each weighted by just two quantities: a geometric factor V_{mn} and a detuning factor d_{mn}. The former is the extent to which the modal pair is excited by a particular temperature profile, while the latter is the combined detuning from the resonances of both modes. Finally, the total spin is a sum over all pairs of modes.

We may apply this understanding to the spin radiation patterns of Figures 3

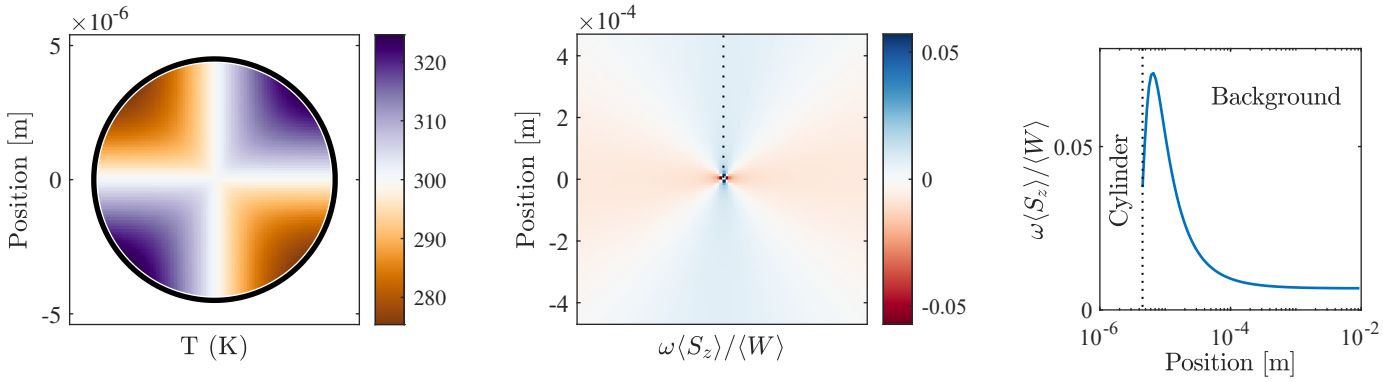

(a) (b) (c)

Figure 4: As in Figure 3, but with a linear temperature profile with four lobes. (a) Temperature profile over the rod cross-section. (b)–(c) Axial spin (normalized by W).

and 4. In this case, cylindrical symmetry is present, so all modes can be assigned an azimuthal variation $\exp(iM\theta)$, for some integer M corresponding to the angular quantum number. In terms of this cylindrical harmonic basis, we observe that if the temperature profile is uniform, then the geometric factor V_{mn} will always vanish for modal pairs with two different values of M. Since two modes with the same M never generate spin when both positive and negative orders are considered, uniform temperature profiles always yield a zero spin field. The same reasoning implies that pure radial gradients of temperature also yield zero spin (not shown).

We now proceed to identify the values of M that do generate spin. In Figure 3, the spin field resembles $\cos\theta$ to lowest order, and is generated by a combination of modes of orders $M = 0$ and $M = \pm 1$. In Figure 4, the spin pattern resembles $\cos 2\theta$, and is generated by modes of orders $M = 1$ and $M = -1$. This difference may mean that the resonance condition for the four-lobe temperature pattern is easier to satisfy, since the resonances of $M = \pm 1$ orders are degenerate. Finally, we may prove that the only component of spin allowed to be non-zero is the z-component. This result holds for infinite rods of any cross-section and any cross-sectional temperature profile, and is proven in Section III Suppl. Mat..

V. OUTLOOK

The modal formalism presented here lays the groundwork for exploring a range of more sophisticated physical scenarios. For example, objects with more complicated shapes (e.g., wires with non-circular cross section, general 3D objects etc.), anisotropy and/or permittivity non-uniformity caused by temperature inhomogeneities [36–38] can be treated using the mode calculation procedure described in [13, 39, 40], known as re-expansion; the symmetry consideration discussed above can be used to deduce the necessary temperature uniformity profile for which spin emission can be realized. Our formulation is also applicable to bound modes below the light line in order to determine the correct near-field emission. Together with unique ability of permittivity mode expansion to treat the interactions between multiple objects (see, e.g., [32, 41, 42]), this allows the thermal emission from multiple interacting structures to be treated, and would be crucial for accurate modelling of near-field heat transfer (see [43]). It would also be an efficient building block in inverse design algorithms aimed at optimizing thermal emission. Finally, our formulation can also be applied to other computationally-heavy problems, such as FRET, quantum friction, and Casimir forces.

The spin emitted by the temperature gradient that we considered is transverse to the Poynting vector. It cannot be measured by traditional approaches based on quarter wave plates, which is only suitable for the measurement of longitudinal spin. Therefore, the experimental detection of such transverse spin would require new approaches such as the one recently proposed for measuring photonic spin density using NV centers [44] or by measuring the resulting torque on levitating nanoparticles [45]. The central result of this work has practical implications for situations requiring non-contact depth-thermography (temperature measurement) based on emitted IR radiation. By comparing the experimental measurements of spin over different emission directions and prior simulation studies (made faster by our modal expansion approach) of the same for various temperature gradient profiles, one can potentially deduce gradient directions. In other words, measurement of photon spin in addition to thermal radiation power can provide valuable additional insight for nanoscale temperature metrology. Fundamentally, the connection between thermal non-equilibria and photon spin is non-intuitive and remains an exciting, unexplored research area.

Acknowledgements. The authors thank N. Shitrit for fruitful and illuminating

discussions. The authors acknowledge funding from the DARPA NLM program.

---

[1] Jean-Jacques Greffet, Patrick Bouchon, Giovanni Brucoli, and Fran çois Marquier. Light emission by nonequilibrium bodies: Local kirchhoff law. *Phys. Rev. X*, 8:021008, Apr 2018.

[2] D. A. B. Miller, L. Zhu, and S. Fan. Universal modal radiation laws for all thermal emitters. *Proc. Nat. Acad. Sci. U.S.A*, 114:4336–4341, 2017.

[3] W. Li and S. Fan. Nanophotonic control of thermal radiation for energy applications. *Optics Express*, 26:15995–16021, 2018.

[4] D. G. Baranov, Y. Xiao, I. A. Nechepurenko, A. Krasnok, Andrea Alú, and M. A. Kats. Nanophotonic engineering of far-field thermal emitters. *Nature Materials*, 18:920–930, 2019.

[5] Jean-Jacques Greffet and Manuel Nieto-Vesperinas. Field theory for generalized bidirectional reflectivity: derivation of helmholtz's reciprocity principle and kirchhoff's law. *JOSA A*, 15(10):2735–2744, 1998.

[6] Andrew Resnick, Chris Persons, and George Lindquist. Polarized emissivity and kirchhoff's law. *Applied optics*, 38(8):1384–1387, 1999.

[7] S.-A. Biehs and P. Ben-Abdallah. Revisiting super-planckian thermal emission in the far-field regime. *Phys. Rev. B*, 93:165405, 2016.

[8] R. M. Abraham Ekeroth, A. García-Martín, and J. C. Cuevas. Thermal discrete dipole approximation for the description of thermal emission and radiative heat transfer of magneto-optical systems. *Phys. Rev. B*, 95:235428, Jun 2017.

[9] Linxiao Zhu, Yu Guo, and Shanhui Fan. Theory of many-body radiative heat transfer without the constraint of reciprocity. *Phys. Rev. B*, 97:094302, Mar 2018.

[10] X. Gao, C. Khandekar, Z. Jacob, and T. Li. Thermal equilibrium spin-torque: Near-field radiative angular momentum transfer in magneto-optical media. *Phys. Rev. B*, 103:125424, 2021.

[11] P. Y. Chen, D. J. Bergman, and Y. Sivan. Generalizing normal mode expansion of electromagnetic Green's tensor to lossy resonators in open systems. *Phys. Rev. Applied*, 11:044018, 2019.

[12] P. Y. Chen and Y. Sivan. Robust location of optical fiber modes via the argument principle method. *Computer Physics Communications*, 214:105–116, 2017.

[13] N. Kossowski, P. Y. Chen, Q. J. Wang, P. Genevet, and Y. Sivan. Generalized normal modes of an anisotropic scatterer. *J. Appl. Phys.*, 129:113104, 2021.

[14] Chihhui Wu, Nihal Arju, Glen Kelp, Jonathan A Fan, Jason Dominguez, Edward Gonzales, Emanuel Tutuc, Igal Brener, and Gennady Shvets. Spectrally selective

chiral silicon metasurfaces based on infrared fano resonances. *Nature communications*, 5(1):1–9, 2014.

[15] SA Dyakov, VA Semenenko, NA Gippius, and SG Tikhodeev. Magnetic field free circularly polarized thermal emission from a chiral metasurface. *Physical Review B*, 98(23):235416, 2018.

[16] Samuel L Wadsworth, Paul G Clem, Eric D Branson, and Glenn D Boreman. Broadband circularly-polarized infrared emission from multilayer metamaterials. *optical materials express*, 1(3):466–479, 2011.

[17] Nir Shitrit, Igor Yulevich, Elhanan Maguid, Dror Ozeri, Dekel Veksler, Vladimir Kleiner, and Erez Hasman. Spin-optical metamaterial route to spin-controlled photonics. *Science*, 340(6133):724–726, 2013.

[18] Tero Setälä, Matti Kaivola, and Ari T Friberg. Degree of polarization in near fields of thermal sources: effects of surface waves. *Physical review letters*, 88(12):123902, 2002.

[19] Chinmay Khandekar and Zubin Jacob. Thermal spin photonics in the near-field of nonreciprocal media. *New Journal of Physics*, 21(10):103030, 2019.

[20] Chinmay Khandekar, Farhad Khosravi, Zhou Li, and Zubin Jacob. New spin-resolved thermal radiation laws for nonreciprocal bianisotropic media. *New Journal of Physics*, 22(12):123005, 2020.

[21] Chinmay Khandekar and Zubin Jacob. Circularly polarized thermal radiation from nonequilibrium coupled antennas. *Phys. Rev. Applied*, 12:014053, Jul 2019.

[22] Alejandro W. Rodriguez, M. T. H. Reid, and Steven G. Johnson. Fluctuating-surface-current formulation of radiative heat transfer: Theory and applications. *Phys. Rev. B*, 88:054305, Aug 2013.

[23] Giuseppe Bimonte, Thorsten Emig, Mehran Kardar, and Matthias Krüger. Nonequilibrium fluctuational quantum electrodynamics: Heat radiation, heat transfer, and force. *Annual Review of Condensed Matter Physics*, 8:119–143, 2017.

[24] Matthias Krüger, Giuseppe Bimonte, Thorsten Emig, and Mehran Kardar. Trace formulas for nonequilibrium casimir interactions, heat radiation, and heat transfer for arbitrary objects. *Phys. Rev. B*, 86:115423, Sep 2012.

[25] Athanasios G. Polimeridis, M. T. H. Reid, Weiliang Jin, Steven G. Johnson, Jacob K. White, and Alejandro W. Rodriguez. Fluctuating volume-current formulation of electromagnetic fluctuations in inhomogeneous media: Incandescence and luminescence in arbitrary geometries. *Phys. Rev. B*, 92:134202, Oct 2015.

[26] Weiliang Jin, Athanasios G. Polimeridis, and Alejandro W. Rodriguez. Temperature control of thermal radiation from composite bodies. *Phys. Rev. B*, 93:121403, Mar 2016.

[27] P. Ben-Abdallah, S.-A. Biehs, and K. Joulain. Many-body radiative heat transfer theory. *Phys. Rev. Lett.*, 107:114301, 2011.

[28] A. Manjavacas and F. J. G. de Abajo. Radiative heat transfer between neighboring

particles. *Physical Review B*, 86:075466, 2012.

[29] S. Sanders, L. Zundel, W. J. M. Kort-Kamp, D. A. R. Dalvit, and A. Manjavacas. Near-field radiative heat transfer eigenmodes. *Physical Review Letters*, 126:193601, 2021.

[30] L. Zhu, S. Sandhu, C. Otey, S. Fan, M. B. Sinclair, and T. S. Luk. Temporal coupled mode theory for thermal emission from a single thermal emitter supporting either a single mode or an orthogonal set of modes. *Appl. Phys. Lett.*, 102:103104, 2013.

[31] M. Zhou, E. Khoram, D. Liu, B. Liu, S. Fan, M. L. Povinelli, and Z. Yu. Self-focused thermal emission and holography realized by mesoscopic thermal emitters. *ACS Photonics*, 8:497–504, 2021.

[32] D. J. Bergman and D. Stroud. Theory of resonances in the electromagnetic scattering by macroscopic bodies. *Phys. Rev. B*, 22:3527–3539, 1980.

[33] L. Novotny and B. Hecht. *Principles of Nano-Optics*. Cambridge University Press, Cambridge, 2006.

[34] L. A. Sphaier, J. Su, R. M. Cotta, and F. A. Kulacki. *Handbook of thermal science and engineering*. Springer, 2017.

[35] V. A. Golyk, M. Krüger, and M. Kardar. Heat radiation from long cylindrical objects. *Phys. Rev. E*, 85, 2012.

[36] P.-T. Shen, Y. Sivan, C.-W. Lin, H.-L. Liu, C.-W. Chang, and S.-W. Chu. Temperature- and -roughness dependent permittivity of annealed/unannealed gold films. *Opt. Exp.*, 24:19254, 2016.

[37] I. Gurwich and Y. Sivan. A metal nanosphere under intense continuous wave illumination - a unique case of non-perturbative nonlinear nanophotonics. *Phys. Rev. E*, 96:012212, 2017.

[38] I. W. Un and Y. Sivan. The thermo-optic nonlinearity of single metal nanoparticles under intense continuous-wave illumination. *Phys. Rev. Mater.*, 4:105201, 2020.

[39] P. Y. Chen, Y. Sivan, and E. A. Muljarov. An efficient solver for the generalized normal modes of non-uniform open optical resonators. *J. Comp. Phys.*, 422:109754, 2020.

[40] P. Y. Chen and Y. Sivan. Resolving Gibbs phenomenon via a discontinuous basis in a mode solver for open optical systems. *J. Comp. Phys.*, 429:110004, 2021.

[41] C. Forestiere, G. Miano, G. Rubinacci, A. Tamburrino, R. Tricarico, and S. Ventre. Volume integral formulation for the calculation of material independent modes of dielectric scatterers. *IEEE Trans. on Ant. and Propagation*, 66:2505, 2018.

[42] G. Rosolen, P. Y. Chen, B. Maes, and Y. Sivan. Overcoming the bottleneck for quantum computations of complex nanophotonic structures: Purcell and förster resonant energy transfer calculations using a rigorous mode-hybridization method. *Phys. Rev. B*, 101:155401, 2020.

[43] S. A. Biehs, R. Messina, P. S. Venkataram, J. C. Cuevas, A. W. Rodriguez, and P. Ben-

Abdallah. Near-field radiative heat transfer in many-body systems. *Reviews of Modern Physics*, 93:025009, 2021.

[44] F. Kalhor, L.-P. Yang, L. Bauer, and Z. Jacob. Quantum sensing of photonic spin density using a single spin qubit. *Phys. Rev. Research*, 3:043007, 2021.

[45] J. Ahn, Z. Xu, J. Bang, P. Ju, X. Gao, and T. Li. Ultrasensitive torque detection with an optically levitated nanorotor. *Nature Nanotechnology*, 15:89–93, 2020.